Novel Zero-Sequence Blocking Transformer (ZSBT) Using Three Single-Phase Transformers

Aitor Laka, *Student Member, IEEE*, Jon Andoni Barrena, *Member, IEEE*, Javier Chivite-Zabalza, Miguel Angel Rodríguez Vidal, *Member, IEEE*, and Gorka Calvo

***Abstract*—Zero-sequence blocking transformers (ZSBTs), used to block the zero-sequence components that are present in a three-phase system, are commonly built winding the three phases around the same core limb. They are difficult to construct, especially in high-power applications that use large cross-sectional cables, as they require a symmetrical winding distribution for not to produce any flux for positive- and negative-sequence components. This paper presents a novel ZSBT configuration using three single-phase transformers. Although slightly greater in size, they can be easily wound, even when thick cables are used. Moreover, the proposed topology can be used as a simulation model of any ZSBT configuration, where core losses and magnetic saturation of the core are included by connecting a single inductor to the secondary windings of the transformers. This paper provides full details of the circuit and is supported by simulation and experimental results of the proposed ZSBT.**

***Index Terms*—AC–DC power converters, blocking transformer, magnetic flux, power harmonic filters, zero sequence.**

I. Introduction

THE zero-sequence blocking transformer (ZSBT) is a magnetic device used to block zero-sequence components. In a three-phase system, these zero-sequence components are defined as the symmetrical components that have the same amplitude and phase in the three phases, also known as common-mode components. The ZSBT imposes a high impedance to the zero-sequence symmetrical components, allowing the flow of balanced positive- and negative-sequence components (also known as differential mode components) by presenting a low impedance to them. Zero-sequence components may appear at the fundamental frequency due to for instance a line imbalance, or can be due to zero-sequence harmonics, those multiple of three (considering a balanced three-phase system), also known as triplen harmonics.

The ZSBTs are typically used in the parallel connection of phase-shifted rectifier units fed by autotransformers to form a multipulse system [1]. They are also used in the parallel connection of inverters where their ac output waveforms have a different instantaneous value, for harmonic cancellation purposes or to avoid the circulation of zero-sequence currents [2]–[5]. An example of parallel connection using a ZSBT is shown in Fig. 1. They can also be connected at the dc side of two parallel-connected rectifiers for the same purpose [6], [7].

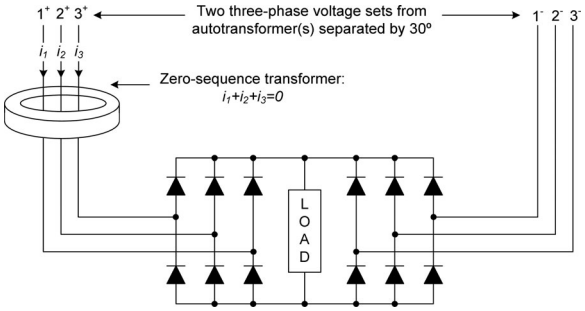

Fig. 1. ZSBT to isolate parallel bridges fed by an autotransformer.

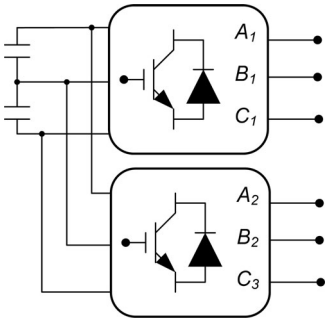

Fig. 2. Three-phase H-bridge with a common dc bus.

Furthermore, there are modulation strategies such as pulsewidth modulation (PWM) with third harmonic injection, full-wave multipulse modulation, or selective harmonic elimination modulation (SHEM), which produce substantial amount of triplen harmonics [8]. This is not usually a concern as these harmonics are naturally canceled out at the output of three-phase systems where the load is connected in delta, or in wye with a floating neutral point. However, this is not always the case [9]–[11]. For instance, if the converter in Fig. 2 is connected to an open winding three-phase output transformer with a low zero-sequence impedance (for instance, wound on a three-limb core, having a zig-zag configuration, or having an auxiliary delta winding), large currents likely to reach fault levels can occur. In these cases, the presence of a ZSBT in the circuit is often used to prevent the circulation of any zero-sequence currents.

This is the case of the convertible static compensator in Fig. 3 [12], where 12 three-level NPC power electronic building blocks (PEBBs) are used, 4 for each phase as can be observed in the

Manuscript received July 18, 2012; revised October 17, 2012; accepted November 14, 2012. Date of publication December 12, 2012; date of current version February 7, 2013. This work was supported in part by the Basque Government under Ph.D. grant program. Paper no. TEC-00380-2012.

A. Laka and J. A. Barrena are with the University of Mondragon, Mondragon 20500, Spain (e-mail: alaka@mondragon.edu; jabarrena@mondragon.edu).

J. Chivite-Zabalza, M. A. R. Vidal, and G. Calvo are with Ingeteam Technology, Zamudio 48170, Spain (e-mail: javier.chivite@ingeteam.com; miguelangel.rodriguez@ingeteam.com; gorka.calvo@ingeteam.com).

Digital Object Identifier 10.1109/TEC.2012.2229282

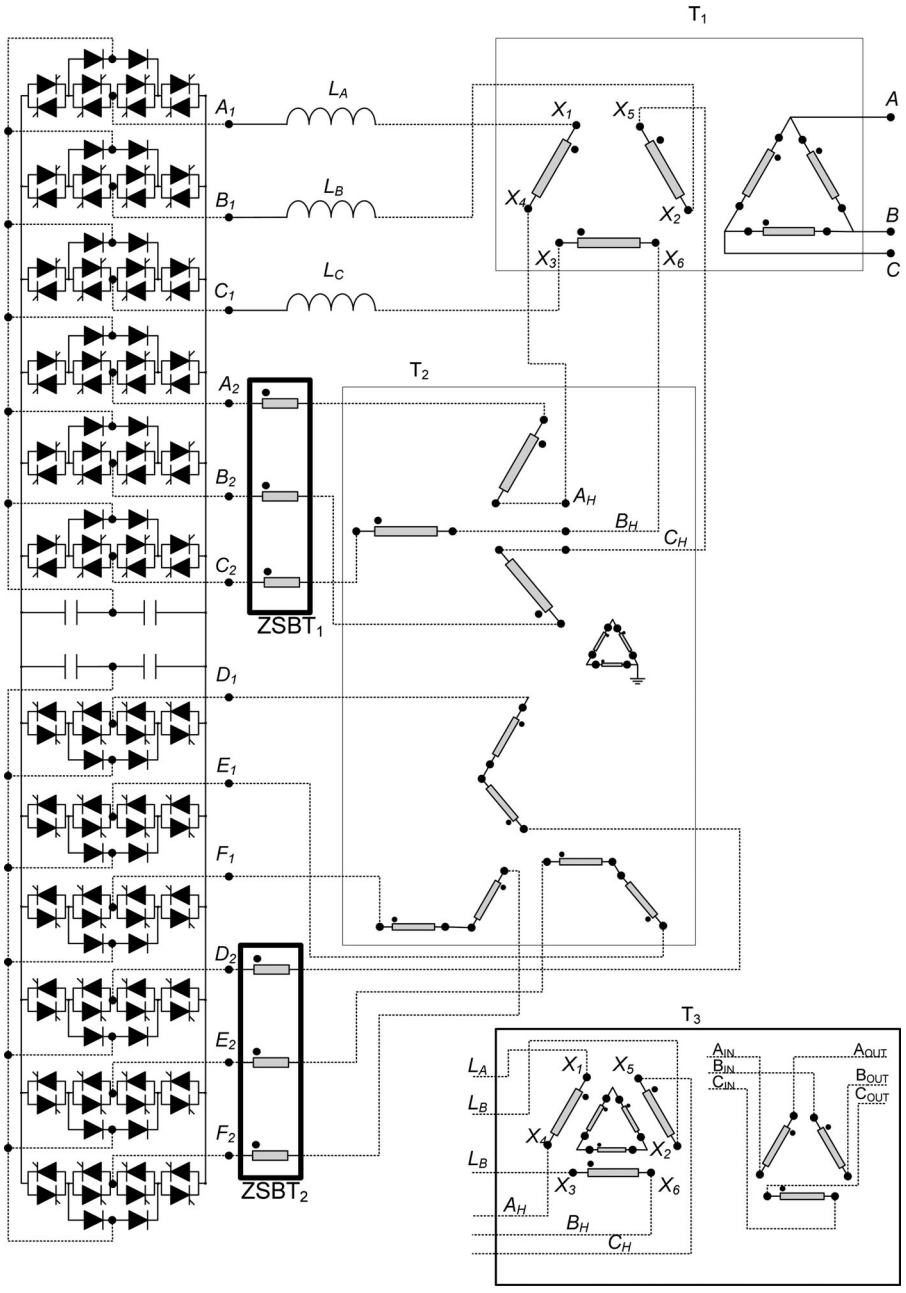

Fig. 3. Power circuit of shunt connected and series connected inverters.

figure. The PEBBs are connected in H-bridge configuration and zero-sequence harmonics are canceled out by using two ZSBTs, the $ZSBT_1$ and the $ZSBT_2$ in Fig. 3.

ZSBTs are typically wound using E cores and toroidal cores. In the former case, they have the three windings wound on the central limb [13], [14]. In the latter case, they are wound on a symmetrical arrangement that keeps them 120° apart from each other. In any case, the inductance that they present to a zero-sequence component is three times the mutual inductance plus any leakage component. Although ZSBTs are intended to block low-frequency harmonics, they are in principle identical to the zero-sequence chokes used for EMI compatibility purposes. However, the design and construction of the latter ones is focused on the high-frequency operating region [15].

The design and construction of a ZSBT is far from being straightforward as it is mandatory to achieve a good flux distribution between different phases so that the net flux produced by a balanced sequence cancels out. Otherwise, the ZSBT could easily saturate. Another important design consideration is that they should withstand the circulation of a small dc current component superimposed to the main currents. This could easily appear unintentionally, created by a small dc voltage offset at the output of the solid-state inverter system. It gets further complicated with high-current, high-power systems, as they require wires with a large cross section that make the winding process even more difficult.

This paper presents a novel ZSBT that employs three single-phase transformers where the primary windings are connected

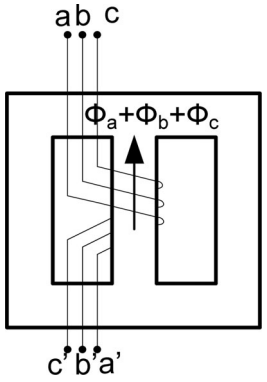

Fig. 4. ZSBT based on an E magnetic core.

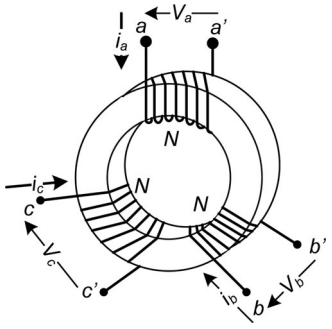

Fig. 5. ZSBT based on a toroidal magnetic core.

in series with the circuit, and the secondary windings are connected in parallel between them. In doing so, they present the self-inductance to the zero-sequence components and the leakage inductance to positive/negative-sequence components. Although the overall size and weight are likely to be slightly greater than those of usual ZSBT configurations, given the higher number of windings and core limbs, this topology may be suitable for high-power applications where usual topologies can be difficult to manufacture. Furthermore, this topology can be used as the simulation model of any kind of ZSBT that incorporates real effects such as core saturation and core losses. This is achieved by adding a saturable inductor, and a core-loss equivalent resistor at the output of the parallel connection of the secondary windings.

The analysis and operation of a conventional ZSBT is described in Section II. The proposed novel ZSBT configuration is presented in Section III, and finally simulation and experimental results of the novel ZSBT are shown, validating the proposed ZSBT configuration.

II. Description of a ZSBT

A. Analysis and Operation of a ZSBT

Typical ZSBTs implemented by using an E core and a toroidal core are shown in Figs. 4 and 5, respectively. In both cases, all the three windings must have the same number of turns.

In both cases, the voltage across any winding, for instance v_a, is calculated by applying Faraday's law:

$$v_a = L\frac{d\,i_a}{dt} + L_o\frac{d\,i_b}{dt} + L_o\frac{d\,i_c}{dt} \tag{1}$$

where L is the self-inductance of phase a, which is assumed to be the same for all windings, and L_o is the mutual inductance between the windings. Equation (1) can also be expressed as:

$$v_a = L_{\rm lk}\frac{d\,i_a}{dt} + L_o\frac{d}{dt}\left(i_a + i_b + i_c\right) \tag{2}$$

where $L_{\rm lk}$ represents the leakage inductance of any winding, which is the difference between the self-inductance L and the mutual inductance L_o.

As mentioned before, the zero-sequence currents have the same phase and amplitude in the three phases. So, they are defined as:

$$i_{\rm ZS} = \frac{(i_a + i_b + i_c)}{3} = i_{a\rm ZS} = i_{b\rm ZS} = i_{c\rm ZS.} \tag{3}$$

Assuming a symmetrical winding distribution, the self-inductance and mutual inductance for all the windings have the same value, and therefore, the current is equally shared. Consequently, by applying (2) and (3), the voltage induced by the zero-sequence currents through the three phases is:

$$v_{\rm ZS} = L_{\rm lk}\frac{d\,i_{\rm ZS}}{dt} + 3L_o\frac{d}{dt}i_{\rm ZS}. \tag{4}$$

It is considered that the mutual inductance is much higher than the leakage inductance. Therefore, neglecting the leakage inductance, the impedance presented by the ZSBT to the zero-sequence components is:

$$Z_{\rm ZS} = \left(L_{\rm lk} + 3L_o\right)\omega \approx 3L_o\omega \tag{5}$$

where ω is the angular frequency.

The differential sequence currents (positive/negative-sequence currents) are the components that form a three-phase balanced set of sinusoidal currents, phase shifted by 120° and having the same magnitude. Therefore, the sum of the instantaneous phase currents is always zero. The impedance presented by the ZSBT to the positive- and negative-sequence currents could be derived from (2):

$$Z_{\rm diff} = L_{\rm lk}\ \omega. \tag{6}$$

Thus, the ZSBT imposes three times the mutual inductance for zero-sequence currents while it imposes the leakage inductance for positive/negative-sequence currents. Note that the mutual inductance is considerable higher than the leakage inductance.

Fig. 6 presents the equivalent magnetic circuit of the conventional ZSBT. It consists of three magnetic forces (one per winding) connected in series to the reluctance of the magnetic core *Ro*. The magnetic flux that flows through the reluctance *Ro* is generated by zero-sequence currents as shown. The magnetic flux generated by positive and negative sequences is closed through the air.

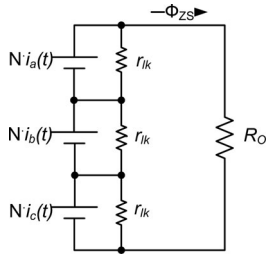

Fig. 6. Equivalent magnetic circuit of a ZSBT.

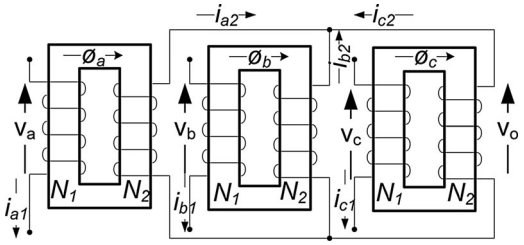

Fig. 7. Configuration of the presented ZSBT.

B. Design Considerations

The main requirement of the ZSBT is the inductance that it has to impose for the zero-sequence currents. The inductance of each phase of the ZSBT is defined by:

$$L_o = \frac{N^2}{Ro} = \frac{N^2}{\frac{l_e}{\mu_0 \mu_r \cdot A}} \tag{7}$$

with N being the turn number of the winding, l_e the length of the magnetic path, and A the cross section of the magnetic core. *Ro* is the reluctance of the magnetic core. It can be observed that the inductance value is directly proportional to the relative permeability value of the core material and the cross section of the core A, quadratically proportional to the number of turns of the winding N, and inversely proportional to the length of the magnetic path l_e.

One of the constraints for the design of the ZSBT is imposed by the saturation of the magnetic core [16]. The maximum flux density flowing through the magnetic core has to be below the saturation point of the B–H curve of the material; otherwise, the impedance of the ZSBT can be drastically reduced generating high zero-sequence currents.

As stated previously, the magnetic flux through the magnetic core is generated only by the zero-sequence currents. The zero-sequence currents can be divided into a dc component and an ac component. From the point of view of the magnetic core saturation, the concern is the peak magnetic flux through the core. This maximum magnetic flux density is generated by the dc and ac components:

$$B_{\max} = B_{\rm dc} + \hat{B}_{\rm ac} \tag{8}$$

with $B_{\rm dc}$ being the magnetic flux density generated by the dc component of the zero-sequence current and $\hat{B}_{\rm ac}$ the amplitude of the magnetic flux density generated by the ac component of the zero-sequence component.

The magnetic force H generated by the dc current component flowing through the windings of the ZSBT can be calculated by:

$$H_{\rm dc} = 3 \cdot \frac{I_{\rm ZSdc} \cdot N}{l_e} \tag{9}$$

where $I_{\rm ZSdc}$ is the dc current component of the zero-sequence currents, N the number of turns of the windings, and l_e the length of the magnetic path. This dc current could easily appear unintentionally, created for example by a small dc voltage offset at the output of a solid-state converter. A small dc voltage offset can generate a relatively high dc current.

The total dc magnetic force is three times the dc magnetic force generated by each phase because they are added in the magnetic circuit as can be seen in Fig. 6. The dc magnetic flux density $B_{\rm dc}$ can be easily obtained from the B–H curve of the material and it is given as:

$$B_{\rm dc} = 3 \cdot \frac{I_{\rm ZSdc} \cdot N}{l_e} \cdot \mu_r \cdot \mu_0. \tag{10}$$

The flux density generated by the ac component of the zero-sequence voltages is:

$$\hat{B}_{\rm ac} = \frac{\hat{V}_{\rm ZS}}{2\pi f} \cdot \frac{1}{N \cdot A} \tag{11}$$

where $V_{\rm ZS}$ is the amplitude of the zero-sequence voltage, N the number of turns of the windings, and A is the cross-sectional area of the magnetic path. Thus, the maximum magnetic flux through the core is given as:

$$B_{\max} = 3 \cdot \frac{I_{\rm ZSdc} \cdot N}{l_e} \cdot \mu_r \cdot \mu_0 + \frac{\hat{V}_{\rm ZS}}{2\pi f} \cdot \frac{1}{N \cdot A}. \tag{12}$$

The design of the ZSBT requires the selection of the material of the magnetic core, the core cross section, the magnetic path length, or the turn number in order to avoid the magnetic core saturation. The magnetic core cross section A can be increased to decrease the ac flux density $B_{\rm ac}$. An increment of the length of the magnetic path l_e implies a decrement of the dc flux density $B_{\rm dc}$. To minimize the effect of the dc current, materials with a relatively low μ_r can be used. In addition, if the turn number N is decreased, the ac flux density will increase whereas the dc flux density will decrease.

Thus, the material and size of the magnetic core, and the turn number of the winding must be defined in order to comply with:

1) the required inductance according to (7);
2) the maximum flux density according to (12), knowing the values of $I_{\rm ZSdc}$ and $\hat{V}_{\rm ZS}$.

III. Proposed Novel ZSBT Using Three Single-Phase Transformers

A. Description of the Presented ZSBT Configuration

A new configuration of the ZSBT that employs three single-phase transformers is presented in this paper. The general scheme of the presented ZSBT is shown in Fig. 7. It consists of three single-phase transformers with the secondary sides connected in parallel, with N_1 turns for the primary-side windings and N_2 for the secondary side.

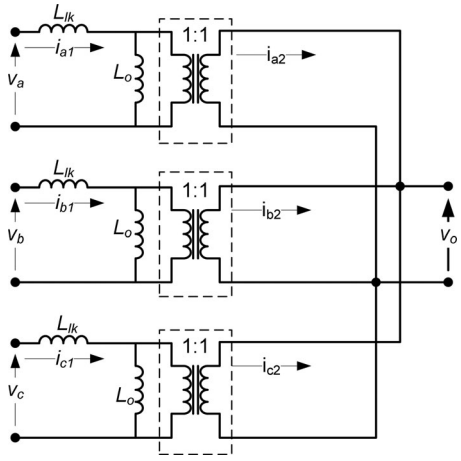

Fig. 8. Three single-phase transformer simplified connection.

The presented ZSBT configuration works as the conventional ZSBTs that are shown in Figs. 4 and 5. It imposes a high impedance for zero-sequence currents and a negligible impedance for differential mode currents. The advantage of the new configuration is the simplicity of the manufacturing, which makes it suitable for high-power applications. In these high-power applications, the current through the ZSBT wires is relatively high, so big cross-sectional cables must be used. So as to ensure that the differential sequence components do not produce any flux, a symmetrical winding distribution is required [17]. Hence, the windings must be wound thoroughly, which is difficult due to the size of the wires. The proposed ZSBT configuration is built using three conventional single-phase transformers making much easier the construction of balanced ZSBTs in these high-power applications.

The equivalent electrical diagram of the ZSBT is shown in Fig. 8 using simplified electrical circuits for the single-phase transformers. $L_{\rm lk}$ is the leakage inductance and L_o is the magnetizing inductance of each single-phase transformer. In order to simplify the analysis, all the resistances have been neglected and it has been considered that the turn ratio of each single-phase transformer is 1:1 ($N_1 = N_2$).

As the secondary sides of the converters are connected in a wye configuration, the sum of the secondary-side currents is zero:

$$i_{a2} + i_{b2} + i_{c2} = 0. \tag{13}$$

The voltage at the secondary side of the transformers v_o can be defined as:

$$\begin{aligned} v_o &= L_o \cdot \frac{d}{dt}\left(i_{a1} - i_{a2}\right) \\ &= L_o \cdot \frac{d}{dt}\left(i_{b1} - i_{b2}\right) = L_o \cdot \frac{d}{dt}\left(i_{c1} - i_{c2}\right). \end{aligned} \tag{14}$$

From (13) and (14), the expression of the voltage v_o is obtained:

$$v_o = \frac{L_o}{3} \cdot \frac{d}{dt}\left(i_{a1} + i_{b1} + i_{c1}\right) \tag{15}$$

where L_o is the magnetizing inductance of the single phase transformer:

$$L_o = \frac{N^2}{R} \tag{16}$$

with N and R being the turn number and the reluctance of the single-phase transformers, respectively.

Having defined the voltage across the secondary sides of the transformers, the voltage of the primary side of the phase a is defined as:

$$v_a = L_{\rm lk} \cdot \frac{d}{dt}\left(i_{a1}\right) + \frac{L_o}{3} \cdot \frac{d}{dt}\left(i_{a1} + i_{b1} + i_{c1}\right). \tag{17}$$

The previous equation is similar to (2) which has been obtained for the conventional ZSBT. So, the impedance imposed by the ZSBT can be deduced in the same way. Combining (3) and (17) and neglecting the leakage inductance, the imposed impedance by the ZSBT to zero-sequence currents is the magnetizing impedance of the single-phase transformer ($Z_{\rm ZS} = \left(L_{\rm lk} + L_o\right)\omega \approx L_o\omega$). For the positive- and negative-sequence components (differential mode components), it could be derived that the imposed impedance is the leakage impedance ($Z_{\rm diff} = L_{\rm lk}\ \omega$).

B. Design Considerations of the Proposed ZSBT

The main requirement of the ZSBT is the inductance that it has to impose for the zero-sequence currents. In this case, the inductance of each phase of the ZSBT is the magnetizing inductance of the single-phase transformer, which can be calculated as in (7):

$$L_o = \frac{N_1^2}{Ro} = \frac{N_1^2}{\frac{l_e}{\mu_0 \mu_r \cdot A}} \tag{18}$$

with N_1 being the turn number of the primary side and *Ro* the reluctance of the magnetic core of the single-phase transformer. Note that the mutual inductance of the ZSBT depends on the turn number of the primary side N_1 and it does not depend on the turn number of the secondary side N_2.

The other requirement that must be taken into account is the maximum flux density of the magnetic core. In (12), the maximum flux density has been obtained for a conventional ZSBT. Similarly, the maximum flux density can be defined for the proposed ZSBT configuration:

$$B_{\max} = \frac{I_{\rm ZSdc} \cdot N_1}{l_e} \cdot \mu_r \cdot \mu_0 + \frac{\hat{V}_{\rm ZS}}{2\pi f} \cdot \frac{1}{N_1 \cdot A}. \tag{19}$$

Observe that the flux density does not depend on the turn number of the secondary-side winding.

So, once defined the size and material of the magnetic core, and the turn number of the primary-side winding N_1 by applying the previous equations, the turn number of the secondary-side winding N_2 must be defined. The current and voltage across the secondary-side windings depend on the turn number N_2. From Fig. 8 and neglecting the magnetizing current, the relation between the primary- and secondary-side currents is obtained:

$$i_{a2} \approx i_{a1} \cdot \frac{N_1}{N_2} \quad i_{b2} \approx i_{b1} \cdot \frac{N_1}{N_2} \quad i_{b2} \approx i_{b1} \cdot \frac{N_1}{N_2}. \tag{20}$$

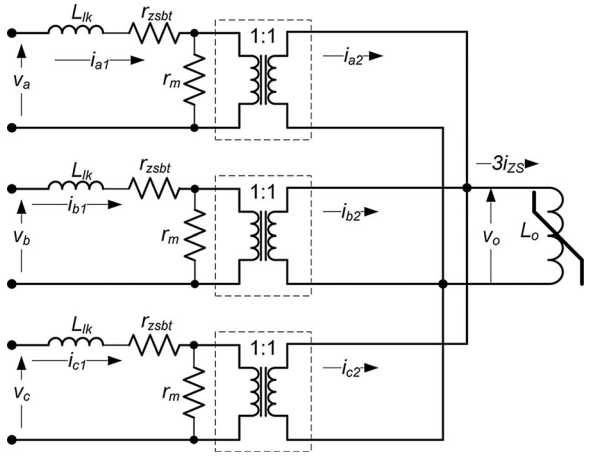

Fig. 9. ZSBT simulation model.

From (15), the voltage across the secondary-side windings is deduced:

$$v_o = L_o \cdot \frac{d\,(i_{\rm ZS})}{dt} \cdot \frac{N_2}{N_1} \approx v_{\rm ZS} \cdot \frac{N_2}{N_1}. \tag{21}$$

Therefore, considering that the turn ratio is 1:1, the secondary-side currents are approximately equal to the primary-side currents, and the secondary-side voltage is also approximately equal to the voltage drop at the primary side of the ZSBT. The current that will flow through the primary of the ZSBT is the load current, so the secondary windings have to be sized to bear this current. In addition, the voltage of the secondary-side windings is only generated by the zero-sequence voltage drop of the ZSBT.

In some high-power applications, these secondary windings should withstand very high currents so on one side very thick cables should be used for these secondary windings, and on the other side there will be high power losses due to the circulation of these secondary currents $(P = I^2R)$. In these applications, as the amplitude of the zero-sequence voltage drop is relatively low, it could be interesting to increase the number of turns of this secondary winding. In doing so, the amplitude of the secondary currents will decrease, reducing the power losses generated by the circulation of these currents on the one hand, and the size of the secondary wires could be reduced on the other.

IV. Simulation Results of the Proposed ZSBT Configuration

The novel ZSBT configuration proposed in this paper could be modeled easily by using the simplified electrical diagram shown in Fig 9. In this simulation model, $r_{\rm zsbt}$ is referred to copper losses, $L_{\rm lk}$ is the leakage inductance, r_m defines the core losses, and core saturation is emulated with a saturable external inductance L_o. Therefore, the proposed ZSBT could be simulated in a simple way.

Moreover, it could be demonstrated that this simulation model could be used to simulate any ZSBT regardless of the used configuration (E core, toroidal core, etc.). For the simulation of conventional ZSBTs as the ones shown in Figs. 4 and 5, three

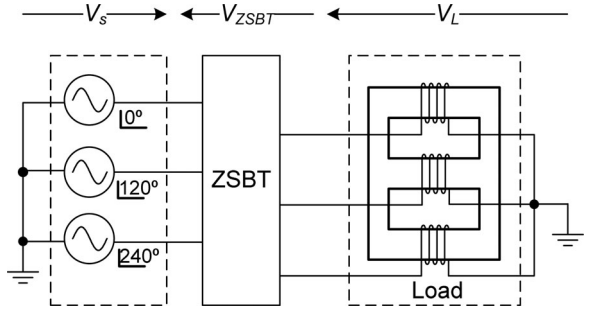

Fig. 10. General test setup.

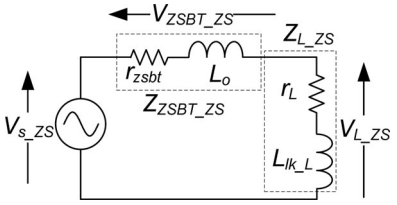

Fig. 11. Equivalent single-phase zero-sequence circuit.

inductors must be coupled magnetically. This issue is not evident at all and convergence or singularity errors can easily occur. Therefore, the simple simulation model presented in Fig. 9 could be used to simulate these conventional ZSBTs as the electrical behavior of the circuit is exactly the same. This simulation model considers the leakage inductance, core losses, copper losses, and core saturation.

The presented configuration of the ZSBT has been validated by a simulation that has been carried out in Saber. The simulated circuit is shown in Fig. 10.

The ZSBT is connected in series between a three-phase voltage source and a three-phase inductive load. The inductive load has been connected in star configuration and its neutral point has been connected to the neutral point of the input voltage source, allowing the circulation of zero-sequence currents.

The inductance of the load L_L is 10 H whereas the leakage inductance $L_{\rm lk\_L}$ and the resistance r_L are 1.5 mH and 1.2 Ω, respectively. In order to build the ZSBT, three single-phase transformers have been used. These transformers have a leakage inductance $L_{\rm lk}$ of 1 mH, a resistance $r_{\rm zsbt}$ of 1 Ω, and a magnetizing inductance L_o of 2.9 H.

For zero-sequence components, the ZSBT imposes the magnetizing impedance and the load imposes the leakage impedance. The equivalent circuit of the test setup for zero-sequence components can be represented as in Fig. 11.

If the ZSBT is not connected, a relatively small common-mode voltage $V_{s\_\rm ZS}$ generates high zero-sequence currents because the load imposes low impedance for zero-sequence components $(Z_{L\_\rm ZS})$. Thus, the connection of the ZSBT is necessary in this kind of applications, where the load presents a very low impedance for these zero-sequence components. For instance, this is the case of a power electronics converter connected to a transformer in star connection with the neutral point connected to the ground. The zero-sequence voltage that the ZSBT must block depends on the amplitude of the zero-sequence voltage

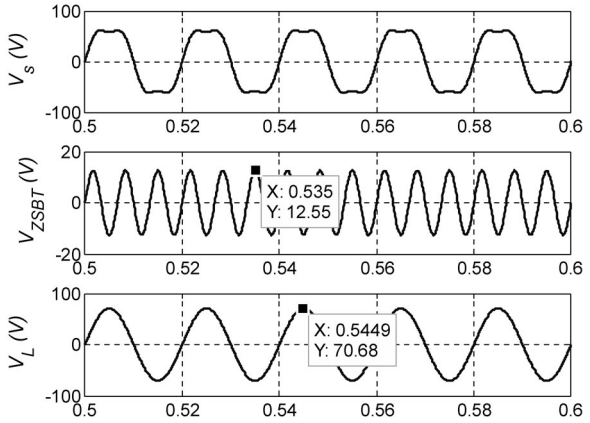

Fig. 12. Simulation results where a third harmonic is added to the fundamental sinusoidal component of the input voltage.

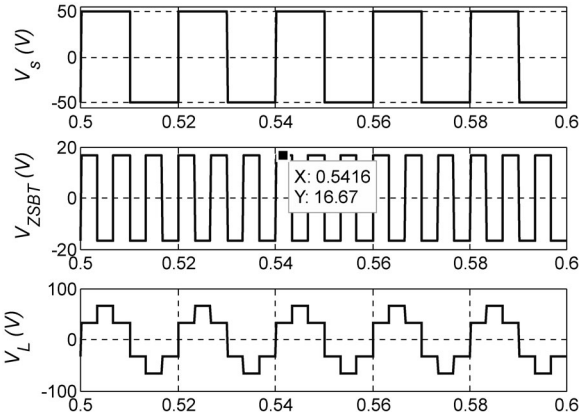

Fig. 13. Simulation results with a square-wave input voltage.

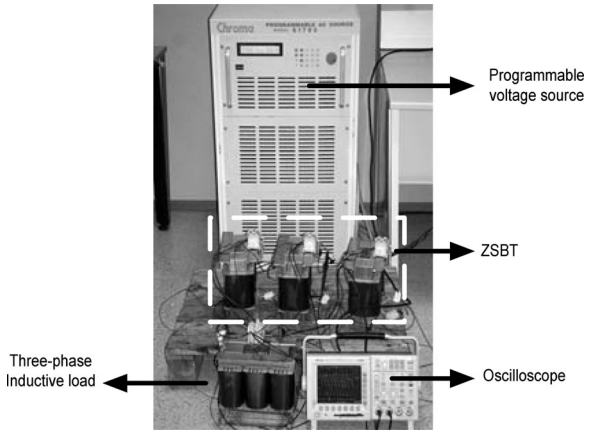

Fig. 14. Experimental test bench.

generated by the converter (V_{s_ZS}), and the imposed impedance for zero-sequence components of the ZSBT $Z_{\mathrm{ZSBT\_ZS}}$ and the load Z_{L_ZS}:

$$V_{\mathrm{ZSBT\_ZS}} = \frac{V_{s\_\mathrm{ZS}}}{Z_{\mathrm{ZSBT\_ZS}} + Z_{L\_\mathrm{ZS}}} \cdot Z_{\mathrm{ZSBT\_ZS}}. \qquad (22)$$

Neglecting the impedance imposed by the load (Z_{L_ZS}) for zero-sequence currents, it can be said that all the zero-sequence voltage of the voltage source drops across the ZSBT. In order to verify it, two different simulations have been carried out. In the first simulation, a three-phase voltage of 50 Vrms and 50 Hz is generated by the voltage source, and a zero-sequence third-harmonic is added to this voltage. The injection of third harmonic is commonly used in PWM modulation techniques to increase the amplitude of the fundamental component. The amplitude of this 150 Hz third harmonic is usually set to 1/6 of the amplitude of the fundamental component [8]. Trying to emulate the behavior of the converter with the injection of third harmonic, the amplitude of the third harmonic component has been set to 17.75% of the amplitude of the fundamental component. The voltages V_s, V_{ZSBT}, and V_L of one of the phases obtained from the simulation are shown in Fig. 12. It can be observed that the zero-sequence component of the voltage V_s drops across the ZSBT and the load is not affected by the third harmonic.

In the second simulation, the voltage source generates a three-phase square waveform (phase-shifted 120° each other) of 50 Hz and 50 V of amplitude. The simulation results are shown in Fig. 13; it can be observed that the zero-sequence component harmonics of the voltage source V_s drop across the ZSBT. As these zero-sequence components are triplen harmonics, they generate a square waveform of three times the fundamental component frequency. Hence, only positive- and negative-sequence components appear in the load voltage V_L.

V. Experimental Results

In order to validate the presented ZSBT configuration, it has been experimentally tested based on the same electrical diagram shown in Fig. 10 that has been simulated in the previous section.

Fig. 14 shows the test bench built at the power electronics laboratory of the University of Mondragon. The input voltage V_s has been generated by using a three-phase programmable Chroma power source, the ZSBT has been built by using three single-phase transformers, and a three-phase inductor connected in star connection has been used as load, connecting the neutral point of the load to the neutral point of the power supply.

As in the previous section, two different tests have been carried out. In the first one, the Chroma power source generates a three-phase voltage that consists of a pure sinusoidal fundamental plus 17.75% of the third harmonic.

The experimental results obtained in this first test are shown in Fig. 15. This figure shows the voltage waveforms measured in one of the phases. The top waveform is the power source voltage, below the ZSBT voltage is shown, and at the bottom the load voltage V_L is displayed.

In the second test, the voltage source generates a three-phase square waveform (phase-shifted 120° each other) of 50 Hz and 50 V of amplitude. The results obtained in the second test are shown in Fig. 16.

It can be observed that the results obtained in the experiments match the simulation results, validating the good behavior of the proposed ZSBT configuration. In addition, the simplicity of the new ZSBT configuration has been verified in the construction

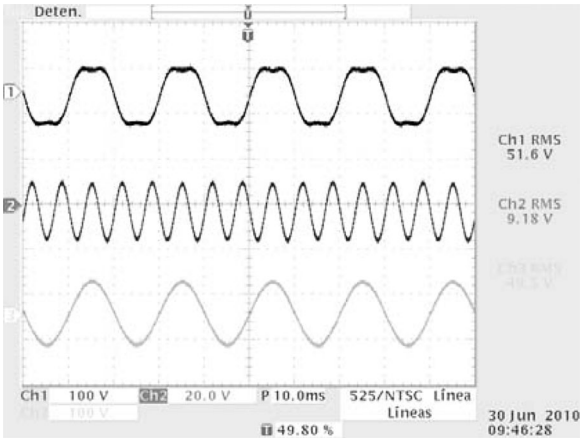

Fig. 15. Results of feeding the ZSBT test circuit with a three-phase sinusoidal waveform with 17.75% of third harmonic. Top waveform: V_s, 100 V/div. Middle waveform: V_{ZSBT}, 20 V/div. Bottom waveform: V_L, 100 V/div.

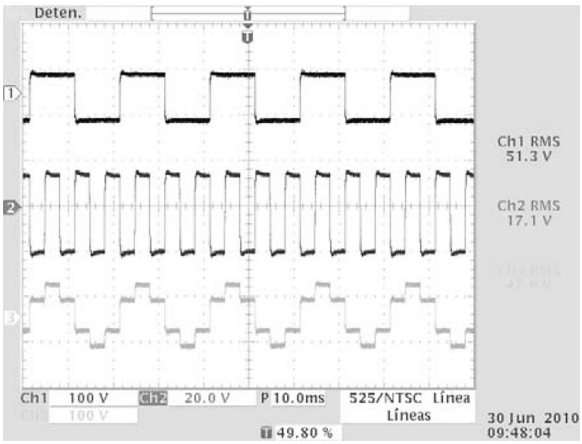

Fig. 16. Results of feeding the ZSBT test circuit with a three-phase square waveform. Top waveform: V_s, 100 V/div. Middle waveform: V_{ZSBT}, 20 V/div. Bottom waveform: V_L, 100 V/div.

of the test bench. It only consists of the interconnection of three single-phase transformers.

VI. Conclusion

This paper presents a novel ZSBT configuration, which is adequate for high-power applications. The high-power ZSBTs are difficult to construct because they use large cross-sectional cables and they require a symmetrical winding distribution for not to produce any flux for positive- and negative-sequence components. The proposed ZSBT configuration is built using three conventional single-phase transformers making much easier the construction of balanced ZSBTs in these high-power applications. The impedance of the ZSBT for zero-sequence components is the magnetizing impedance of the single-phase transformer and the impedance for positive- and negative-sequence components is the leakage impedance of the single-phase transformer.

The new configuration can be used also as a simulation model taking into account the leakage inductance, the core losses, the copper losses, and the core saturation. This simulation model is easier to simulate because three single-phase transformers are used instead of three coupled inductors.

Although the overall size and weight are likely to be slightly greater than those of usual ZSBT configurations, given the higher number of windings and core limbs, this topology may be suitable for high-power applications where usual topologies can be difficult to manufacture.

The new configuration of the ZSBT has been simulated and experimentally tested. These simulation and experimental results are presented in this paper, verifying the good performance of the proposed ZSBT configuration.

References

[1] D. A. Paice, *Power Electronic Converter Harmonics*. Piscataway, NJ: IEEE Press, 1996, p. 88.

[2] J. Chivite-Zabalza, M. Rodriguez, P. Izurza, G. Calvo, and D. Madariaga, "A large power voltage source converter for FACTS applications combining 3-level neutral point clamped power electronic building blocks," *IEEE Trans. Ind. Electron.*, pp. 1–1, 2012.

[3] L. Asiminoaei, E. Aeloiza, P. N. Enjeti, and F. Blaabjerg, "Shunt active-power-filter topology based on parallel interleaved inverters," *IEEE Trans. Ind. Electron.*, vol. 55, no. 3, pp. 1175–1189, Mar. 2008.

[4] B. Cougo, T. Meynard, and G. Gateau, "Parallel three-phase inverters: Optimal pwm method for flux reduction in intercell transformers," *IEEE Trans. Power Electron.*, vol. 26, no. 8, pp. 2184–2191, Aug. 2011.

[5] L. Asiminoaei, E. Aeloiza, J. H. Kim, P. Enjeti, F. Blaabjerg, L. T. Moran, and S. K. Sul, "Parallel interleaved inverters for reactive power and harmonic compensation," in *Proc. 37th IEEE Power Electron. Spec. Conf.*, 2006, pp. 1–7.

[6] B. Singh, "An autotransformer-based 36-pulse controlled ac–dc converter," *IETE J. Res.*, vol. 54, no. 4, 2008.

[7] C. M. Young, M. H. Chen, C. H. Lai, and D. C. Shih, "A novel active interphase transformer scheme to achieve three-phase line current balance for 24-pulse converter," *IEEE Trans. Power Electron.*, vol. 27, no. 4, pp. 1719–1731, Apr. 2012.

[8] D. G. Holmes and T. A. Lipo, *Pulse Width Modulation For Power Converters*. Piscataway, NJ: IEEE Press, 2003, p. 221.

[9] B. Singh and S. Gairola, "A 40-pulse AC–DC converter fed vector-controlled induction motor drive," *IEEE Trans. Energy Convers.*, vol. 23, no. 2, pp. 403–411, Jun. 2008.

[10] D. Graovac, T. Hoffmann, and A. Haltmair, "A transfer function approach to a common mode filter (CMMF) optimization in the PWM inverter supplied motor drives," *IEEE Trans. Energy Convers.*, vol. 26, no. 4, pp. 93–101, Mar. 2011.

[11] L. Asimmoaei, E. Aeloiza, J. H. Kim, P. Enjeti, F. Blaabjerg, L. T. Moran, and S. K. Sul, "An interleaved active power filter with reduced size of passive components," in *Proc. 21st Annu. IEEE Appl. Power Electron. Conf. Expo.*, 2006, p. 8.

[12] Convertible Static Compensator (CSC) for New York Power Authority, EPRI, Palo Alto, CA, and New York Power Authority, White Plains, NY, 2001, 1001970.

[13] S. Qipeng, Y. Zhongdong, X. Jinhui, and Z. Lixia, "Zero-sequence harmonics current minimization using zero-blocking reactor and zig-zag transformer," in *Proc. 3rd Int. Conf. Elect. Utility Deregulation Restruct. Power Technol.*, 2008, pp. 1758–1764.

[14] D. A. Paice, "Low kVA/kW transformers for AC to DC multipulse converters," U.S. Patent 7 233 507, Jun. 19, 2007.

[15] P. S. Chen and Y. S. Lai, "Effective EMI filter design method for three-phase inverter based upon software noise separation," *IEEE Trans. Power Electron.*, vol. 25, no. 11, pp. 2797–2806, Nov. 2010.

[16] D. Zhang, F. Wang, R. Burgos, and D. Boroyevich, "Total flux minimization control for integrated inter-phase inductors in paralleled, interleaved three-phase two-level voltage-source converters with discontinuous space-vector modulation," *IEEE Trans. Power Electron.*, vol. 27, no. 4, pp. 1679–1688, Apr. 2012.

[17] J. M. C. Rodriguez, G. A. Orcajo, C. H. R. Garcia, M. G. Melero, M. F. Cabanas, and F. P. Gonzalez, "Analysis of the effects caused by structural asymmetries in the performance of three-limb core three-phase inductive filters," *IEEE Trans. Energy Convers.*, vol. 22, no. 3, pp. 600–607, Sep. 2007.

Aitor Laka (S'10) was born in Gernika, Spain, in 1985. He received the B.S. and M.S. degrees in electronics engineering from the University of Mondragon, Mondragon, Spain, in 2006 and 2009, respectively, where he is currently working toward the Ph.D. degree.

His research interests include power electronics, multilevel topologies, distributed generation, and renewable energy.

Jon Andoni Barrena (M'04) received the B.Sc. degreee in electronics from the University of Mondragon, Mondragon, Spain, in 2000, the M.Sc. degree (with distinction) from the University of Manchester Institute of Science and Technology, Manchester, U.K., in 2011, and the Ph.D. degree from the University of Mondragon, in 2007.

Since 2001, he has been a Lecturer at the University of Mondragon. His research interests include power electronics, grid quality, distributed generation, and renewable energy.

Javier Chivite-Zabalza received the B.Sc. Eng. degree in electrical and electronic engineering from Mondragon University, Mondragon, Spain, the M.Sc. degree in power electronics and drives from the Universities of Birmingham and Nottingham (joint degree), Birmingham, U.K., and the Ph.D. degree from the University of Manchester, Manchester, U.K., in 1993, 2003, and 2006, respectively.

He was a Project Engineer in the field of industrial automation and drives from 1994 to 1999 in Spain, and from 1999 to 2003 in the U.K. From 2003 to 2006, he was with Goodrich ESTC, Birmingham, where he was involved in the development of high power-factor rectifiers for aerospace applications. From 2006 to 2008, he was with the Rolls-Royce University Technology Centre, University of Manchester, where he was involved in research on more electric concepts for autonomous aerospace power systems. In 2008, he joined Ingeteam Technology S.A., Zamudio, Spain, where he is developing power electronic converters for FACTS devices and motor drives applications. He is currently in charge of the Voltage Source Converter development for the 47 MVAR SSSC demonstrator.

Dr. Chivite-Zabalza is a Registered Chartered Engineer in the U.K. and a member of the Institution of Engineering and Technology.

Miguel Angel Rodríguez Vidal (M'06) was born in San Sebastian, Spain, in August 1966. He received the B.Sc. (Eng.) degree in electronic engineering from Mondragon University, Mondragon, Spain, the M.Sc. degree in electrical engineering from the Swiss Federal Institute of Technology, Lausanne, Switzerland, and the Ph.D. degree in industrial engineering from the University of Zaragoza, Saragossa, Spain, in 1989, 1992, and 2000, respectively.

From 1992 to 2008, he was an Associate Professor in the Electronics Department of the University of Mondragon and participated in different research projects in the field of wind energy systems, lift drives, and railway traction. In September 2008, he joined Ingeteam. He is currently the Power Electronics Systems Manager at the Power Grid Automation business unit of Ingeteam Power Technology, Zamudio, Spain, where he is responsible for developing new power electronics solutions for transmission and distribution grid applications. His research interest includes modeling and control of voltage source converters for FACTS applications such as SSSC, STATCOM, and energy storage systems, and the grid integration studies for those systems.

Gorka Calvo received the B.Sc. degree in electronics engineering from the Escuela de Ingeniería Técnica Industrial de Bilbao, Bilbao, Spain, in 2005, and the M.Sc. degree in automatics and industrial electronics from the Escuela Técnica Superior de Ingeniería de Bilbao, Bilbao, in 2009.

From 2007 to 2009, he was with Supsonik S.L, Sondika, Spain, as an RDi Engineer of power electronics, designing and testing hardware and control of rectifiers, UPS, voltage-frequency converters and PV inverters. Since 2009, he has been with Ingeteam Power Technology S.A., Zamudio, Spain, where he is involved in high-voltage and high-power converters, for industrial and FACTs applications. His research interests include power electronics, control of power converters, modeling of power converters, and alternative energy systems.